Identification of a Xylogalacturonan Xylosyltransferase Involved in Pectin Biosynthesis in Arabidopsis [W OA]

Jacob Kru¨ ger Jensen,[a] Susanne Oxenbøll Sørensen,[a] Jesper Harholt,[a] Naomi Geshi,[a] Yumiko Sakuragi,[a] Isabel Møller,[b] Joris Zandleven,[c] Adriana J. Bernal,[b] Niels Bjerg Jensen,[a] Charlotte Sørensen,[a] Markus Pauly,[d] Gerrit Beldman,[c] William G.T. Willats,[b] and Henrik Vibe Scheller[a,e,1]

[a] Laboratory of Molecular Plant Biology, Department of Plant Biology, Faculty of Life Sciences, University of Copenhagen, DK-1871 Frederiksberg C, Denmark

[b] Department of Molecular Biology, Faculty of Science, University of Copenhagen, DK-1353 Copenhagen, Denmark [c] Laboratory of Food Chemistry, Department of Agrotechnology and Food Sciences, Wageningen University, 6700 EV Wageningen, The Netherlands

[d] Max Planck Institute for Molecular Plant Physiology, D-14476 Golm, Germany [e] Feedstocks Division, Joint Bioenergy Institute, Emeryville, California 94608

Xylogalacturonan (XGA) is a class of pectic polysaccharide found in plant cell walls. The Arabidopsis thaliana locus At5g33290 encodes a predicted Type II membrane protein, and insertion mutants of the At5g33290 locus had decreased cell wall xylose. Immunological studies, enzymatic extraction of polysaccharides, monosaccharide linkage analysis, and oligosaccharide mass profiling were employed to identify the affected cell wall polymer. Pectic XGA was reduced to much lower levels in mutant than in wild-type leaves, indicating a role of At5g33290 in XGA biosynthesis. The mutated gene was designated xylogalacturonan deficient1 (xgd1). Transformation of the xgd1-1 mutant with the wild-type gene restored XGA to wild-type levels. XGD1 protein heterologously expressed in Nicotiana benthamiana catalyzed the transfer of xylose from UDP-xylose onto oligogalacturonides and endogenous acceptors. The products formed could be hydrolyzed with an XGA-specific hydrolase. These results confirm that the XGD1 protein is a XGA xylosyltransferase. The protein was shown by expression of a fluorescent fusion protein in N. benthamiana to be localized in the Golgi vesicles as expected for a glycosyltransferase involved in pectin biosynthesis.

INTRODUCTION

The plant cell wall provides support, defines cell and plant shape, and serves as a barrier against pathogens and the environment. Although extracellular, cell walls are strong yet responsive, highly dynamic structures that allow cell expansion and division. Plant cell walls are composed mostly of polysaccharides but also contain proteins, glycoproteins, and, in certain cells, lignin. Different classes of polysaccharides are present in cell walls: microfibrils of cellulose are imbedded in a polymer matrix, the nature of which varies across plants and cell types. The primary walls of growing cells typically contain approximately equal amounts of cellulose, pectin, and hemicelluloses; xyloglucan is the most abundant hemicellulose in most plants. By contrast, grasses and other commelinoids have somewhat different walls, with a lower content of pectin and an abundance of arabinoxylan rather than xyloglucan. Pectin is a complex group of polysaccharides that are characterized by a high content of galacturonic acid and are relatively soluble. The major classes of pectic poly-saccharides are homogalacturonan (HG), rhamnogalacturonan I (RGI), rhamnogalacturonan II (RGII), and xylogalacturonan (XGA) (Willats et al., 2001). Some pectic domains are likely to be cova-lently linked in the wall (Ishii and Matsunaga, 2001; Nakamura et al., 2002). HG is composed of a linear chain of a-1,4-linked GalA residues that are often methylesterified on C6 and can be acetylated on C2 and/or C3. RGI consists of a backbone with the disaccharide [a-1,4-GalA-a-1,2-Rha] as the basic repeating unit. Rhamnose residues in RGI are often substituted with side chains of galactan, arabinan, or arabinogalactan I, although RGI struc-tures are highly complex and variable (for a review, see Mohnen 1999). RGII is a polysaccharide with a complex structure that appears to be remarkably conserved in all vascular plants (Matsunaga et al., 2004; O'Neill et al., 2004). RGII consists of a short stretch of HG substituted with four different side chains and is composed of 12 different monosaccharides in >20 different linkages. XGA consists of a HG backbone that it is substituted with single b-1,3-Xyl residues or such residues substituted with a few additional xylose residues (Zandleven et al., 2006). XGA has been reported especially in reproductive tissues but is probably present in all tissues (Zandleven et al., 2007).

Pectin is synthesized by enzymes located in Golgi vesicles. Based on structural analysis, >50 different transferase activities are needed to synthesize pectin; most of these enzymes are glycosyltransferases, but methyl- and acetyltransferases are also needed (Mohnen, 1999). Two transferase activities have been unambiguously assigned to specific proteins: GAUT1 is a galacturonosyl transferase that can extend HG (Sterling et al., 2006), and RGXT1 and RGXT2 are isoforms of a xylosyltransfer-ase that can transfer xylose onto the A-chain of RGII (Egelund et al., 2006). Putative pectin biosynthetic enzymes include ARAD1, which is likely to be directly involved in synthesizing arabinan (Harholt et al., 2006), although the activity of the enzyme has not been demonstrated. GUT1 is reported to be involved in transfer of glucuronic acid onto side chain A of RGII in *Nicotiana peruvianum*, but the specificity of the enzyme is uncertain since the mutant lacking the enzyme has a more general deficiency in glucuronic acid (Iwai et al., 2002, 2006). QUA1 has sequence similarity to GAUT1 and plays a role in pectin biosynthesis (Bouton et al., 2002), although the activity has not been demonstrated and the mutant phenotype is pleiotropic (Orfila et al., 2005). For a recent review on pectin biosynthesis, see Scheller et al. (2007).

Glycosyltransferases have been classified by Coutinho and Henrissat (1999) according to their domain structure into 91 different families, of which 40 are represented in *Arabidopsis thaliana*. The members of the different glycosyltransferase fam-ilies can be conveniently accessed

through the CAZy database (http://www.cazy.org). Some families are particularly highly rep-resented in plants, suggesting that many of their members are responsible for plant-specific functions (Scheller et al., 2007). These families include CAZy glycosyltransferase Families 2, 4, 8, 47, and 77. While Family 4 contains many enzymes involved in starch and sucrose metabolism, the other four families have all been shown to contain members involved in cell wall biosynthe-sis. Family 2 includes cellulose synthase and cellulose synthase– like proteins, many of which have already been demonstrated to play a role in cell wall biosynthesis. Family 8 includes GAUT1 and QUA1, while Family 77 includes RGXT1 and RGXT2. Family 47 has 39 members in *Arabidopsis* and includes ARAD1 and At5g61840, the closest homolog of *N. peruvianum* GUT1 men-tioned above. Family 47 also includes MUR3, which is a galacto-syltransfease involved in xyloglucan biosynthesis (Madson et al., 2003), FRA8, which is involved in xylan biosynthesis (Zhong et al., 2005), and IRX10 (At1g27440; Brown et al., 2005). Thus, Family 47 has proven to be a highly interesting group of enzymes, many (perhaps all) of which play a role in cell wall biogenesis. To investigate the role of some of these enzymes, we analyzed cell wall composition in insertional mutants of *Arabidopsis*. Here, we describe a mutant with decreased XGA. Based on the cell wall phenotype and the enzymatic activity of the corresponding pro-tein, we conclude that the mutated gene encodes an XGA-specific xylosyltransferase.

RESULTS

At5g33290 Encodes a Putative Glycosyltransferase

The locus of At5g33290 has an open reading frame made up of four exons (Figure 1). The gene structure is supported by isola-tion of full-length cDNA clones (e.g., GenBank accession number BX831739 originating from Genoscope, Centre National de The intron-exon structure of the At5g33290 locus is indicated (introns are drawn as thin lines and exons as gray bars), and the positions of the T-DNA insertions in *xgd1-1* and *xgd1-2* are marked (triangles). The positions of the primers (arrows) used for screening by PCR and for RT-PCR analysis of transcript levels are shown. The left RT-PCR primer contains exon sequence spanning an intron; the omitted intron sequence is indicated by a dashed line.

Sequencage, Evry, France). The encoded protein of 500 amino acid residues is calculated to have a polypeptide molecular mass of 56.6 kD. The protein is predicted to be targeted to the secretory pathway and to have a signal anchor with a single transmembrane helix from residues 9 to 31. These features are typical for a Type II membrane protein. Sequence similarity to other CAZy Family 47 proteins suggests that the protein is an inverting glycosyltransferase. Inverting glycosyltransferases in-vert the configuration of the anomeric carbon in the nucleotide sugar substrate (i.e., they generate b-linkages with most nucleo-tide sugar substrates). The protein has four sites predicted by NetNGlyc to be *N*-glycosylated. Based on the data reported below, we designate the protein XYLOGALACTURONAN DEFI-CIENT1 (XGD1).

Identification of Two T-DNA Insertion Lines in XGD1

Two independent T-DNA insertion lines in *XGD1* were obtained from the Syngenta SAIL collection and from SALK (Figure 1). The two mutant lines are designated *xgd1-1* and *xgd1-2*. Homozy-gous lines were identified by PCR. For *xgd1-1*, PCR yielded a product of expected size consistent with location of the T-DNA as indicated in the database (Figure 1). However, in the case of *xgd1-2*, the insert proved to be located ;400 bp downstream of the position reported by SALK. Consequently, the T-DNA inser-tion of *xgd1-2* was concluded to be located 90 bp upstream of the stop codon of *XGD1*, as verified by sequencing. This insertion leads to substitution of the last 30 amino acid residues of the XGD1 protein (see Supplemental Figure 1 online) and hence alters the highly conserved C-terminal region of the protein.

The insertion lines were investigated using real-time RT-PCR (Table 1). For *xgd1-1*, no transcript was detected, but for *xgd1-2*, the disruption of the gene did not lead to any significant desta-bilization of the *xgd1-2* mRNA.

Expression Analysis of XGD1

We analyzed the expression pattern of *XGD1* in stems, adult leaves, juvenile leaves, and roots by real-time RT-PCR (Table 1). *XGD1* is most highly expressed in adult leaves and at twice the level found in juvenile leaves. In stems and roots, the transcript level is 8.2 and 5.4%, respectively, compared with the level in adult leaves. These findings are in good agreement with data Xylogalacturonan Biosynthesis from publicly available array experiments, except that we found a lower expression in roots than reported in other experiments. Analysis of public array data (see Supplemental Figure 2 online) showed that expression of *XGD1* is highly increased by biotic stresses, such as infection with *Botrytis* and *Pseudomonas*, and abiotic stresses, such as nutrient deficiency, whereas infection with *Agrobacterium tumefaciens* or nematodes decreases *XGD1* expression. Furthermore, the expression is strongly increased by senescence and decreased by cytokinin (benzyladenine).

T-DNA Insertions in XGD1 Cause a Decrease in Cell Wall Xylose

Since Family 47 glycosyltransferases are likely to be involved in cell wall biosynthesis (Scheller et al., 2007), we determined the effect of insertional mutagenesis of *XGD1* on the monosaccha-ride composition of cell wall material isolated from adult leaves obtained from *xgd1-1* and *xgd1-2* (Figure 2; typical chromato-grams are shown in Supplemental Figure 3 online). A reduction of ;25% in the xylose content was observed for both *xgd1-1* and *xgd1-2*, whereas no other monosaccharides were significantly altered. The reduction in xylose in the *xgd1* mutants was con-sistently observed in all experiments performed and varied from ;15 to 30% between experiments. Neither the *xgd1-1* plants nor the *xgd1-2* plants displayed any visible difference in growth phenotypes compared with *quartet*

(*qrt*) and Columbia-0 (Col-0), respectively. The *xgd1-1* mutant is, like other mutants in the Syngenta SAIL collection, made in the *qrt* genetic background. Recently, *qrt* was shown to encode a pectin methylesterase, but it is primarily expressed in pollen grains and is not expressed in leaves and stems (Francis et al., 2006). The *qrt* and Col-0 lines were indistinguishable in monosaccharide composition in the tissues investigated in this study and also did not differ in growth phenotype. Therefore, *qrt* is considered the wild type in this study.

Several cell wall polymers contain xylose to varying degrees, including xyloglucan, xylan, XGA, and RGII. A range of approaches were used to determine in which polymer xylose was reduced.

Immunomicrodot assays using cell wall–specific antibodies (mAbs) were performed to probe the relative levels of galactan (mAb LM5), arabinan (mAb LM6), xyloglucan (mAb CCRC-M1), and xylan (mAb LM11) in a range of organs/tissues in the wild type (i.e., *qrt*) and *xgd1-1*. This analysis did not reveal any significant differences in the levels of the investigated polymers in any of the samples tested (data not shown).

Although not extensively characterized, XGA is another xylose-containing polymer in *Arabidopsis* cell walls (Zandleven et al., 2007). Presently, the amount of XGA in the walls cannot be accurately determined, but the study by Zandleven et al. (2007) showed that up to 7% of the pectin from leaves could be hydrolyzed by the specific enzyme XGA hydrolase.

To identify the affected polymer in the mutant, we treated cell wall material from leaves with endopolygalacturonase and pectin methylesterase and analyzed the monosaccharide content in the extracted pectin fraction and in the remaining residue (Figure 3; typical chromatograms are shown in Supplemental Figure 4 online). This analysis demonstrated that there was no difference in the xylose content in the residue between the wild type (*qrt*) and *xgd1-1*. The extraction of pectin was equally efficient in both genotypes, with 62% of the rhamnose and 91% of the galactur-onic acid released. The stochiometric Rha/GalA ratio in the pellets was near 1 in both the wild type and *xgd1-1*, indicating that a near to total extraction of HG and XGA was achieved, while approximately one-third of the RGI remained in the pellet.

To further investigate the pectin, we purified the high molecular mass fraction representing RGI and XGA from the released material. The monosaccharide composition analysis of the iso-lated RGI/XGA showed a substantial decrease from 3.8 to 1.2 mol % (i.e., percentage of total monosaccharide content on a molar basis) of xylose in the *xgd1-1* mutant compared with the wild type (Table 2; typical chromatograms are shown in Supple-mental Figure 5A online). Consistently, a 76% reduction of terminal xylose was observed in the same fraction (from 4.6 to

Cell wall material (alcohol insoluble residue) was isolated from leaves, hydrolyzed with trifluoroacetic acid, and analyzed by high-performance anion exchange chromatography with pulsed amperometric detection (HPAEC-PAD). Monosaccharide content is expressed as mean mol % 6 SD (*n* ¼ 3 independent samples). The *xgd1-1* and *xgd1-2* mutants had significantly lower xylose content than the corresponding wild types (two-way analysis of variance [ANOVA], $P < 10^{3^5}$). No other monosac-charide was significantly changed in the mutants ($P > 0.05$). The xylose content in the two sample sets (*qrt*/*xgd1-1* and Col-0/*xgd1-2*) was indistinguishable (two-way ANOVA, $P > 0.1$. Pectin was extracted from cell wall material from rosette leaves from the wild type (*qrt*) and *xgd1-1* by the action of polygalacturonase and pectin methylesterase. The extracted pectin and the residue were hydrolyzed with trifluoroacetic acid, and the monosaccharide composition was analyzed by HPAEC-PAD. The data are expressed as mean mol % 6 SD (*n* ¼ 3 independent samples). The xylose content in the extracted pectin is significantly lower than in the wild type (*t* test, $P < 0.0001$), whereas the residue showed no difference in xylose content (*t* test, $P > 0.7$).

1.1 mol %; Table 2), clearly indicating a significant reduction of the xylose substituted HG (i.e., XGA). Monosaccharide analysis also indicated a reduction in GalA from 37.9 to 30.8%. This is in agreement with the reduced xylose assuming a Xyl/GalA ratio in XGA of ;1:3. Notably, the monosaccharide and linkage analy-ses confirmed the absence of 2-Xyl, 4-Xyl, and Glc, proving that the RGI/XGA preparations did not contain any detectable hem-icellulose contamination. To investigate linkage of uronic acids, we conducted a separate linkage analysis after reduction of uronic acids (typical chromatograms shown in Supplemental Figure 5B online). The procedure is not optimal for determining content of neutral sugars; therefore, the results were obtained independently. To more easily compare the data, they have been compounded into one table (Table 2). The data showed a 2.1 mol % decrease in the content of branched GalA residues, 3,4-GalA, in the mutant in agreement with the reduction in terminal xylose. Interestingly, the ratio of 2-Rha (non–side chain RGI residue) and 2,4-Rha (side chain containing RGI residue) was altered (Table 2). In the wild type (*qrt*), 35% of Rha was in the 2,4-Rha form, indicating that on average approximately every third rhamnose residue had a side chain. In the mutant, the 2,4-Rha constituted 45%. Hence, RGI of *xgd1-1* contains a more highly substituted RGI chain. This is consistent with an increase in galactose in the RGI/XGA fraction (38% in the monosaccharide compositional analysis) and of 4-Gal and t-Gal in the linkage analysis (44 and 23% increase, respectively), suggesting an increase in pectic galactan in this enzyme solubilized fraction.

The Decrease in Xylose Is Due to a Decreased Content of XGA

The highly decreased content of terminal xylose residues in pectin isolated from *xgd1-1* indicated that XGA was the affected polymer. To specifically compare the presence of XGA in the cell wall of wild-type (*qrt*) and *xgd1-1* plants, we used XGA hydrolase, a highly specific enzyme that has no detectable activity with HG or any other pectic polysaccharide besides XGA (Zandleven et al., 2007). XGA hydrolase accepts xylosylated GalA residues in both ₃1 and þ1 positions; hence, the product of XGA digestion with the enzyme is a mixture of xylogalacturonides and oligoga-lacturonides (Zandleven et al., 2007). A pectin-enriched fraction from wild-type and *xgd1-1* plants was treated with XGA hydrolase and subsequently analyzed by HPAEC-PAD and matrix-assisted laser-desorption ionization time of flight mass spectrometry (MALDI-TOF MS) (Figure 4). Nine different oligosaccharides, including the isomer $GalA_2Xyl$', could be identified in the enzy-

matically treated pectin fraction obtained from wild-type plants, whereas no oligosaccharides were detected from *xgd1-1*. Some XGA could also be detected in the residue after pectin extraction in the wild type, but no XGA-derived oligomers could be detected in *xgd1-1* residue. As expected (Zandleven et al., 2007), the main

functional XGD1 protein is directly responsible for the decreased XGA content. To further substantiate this, we performed a complementation experiment. In *xgd1-1* plants that were trans-formed with a construct carrying *XGD1* under control of the cauliflower mosaic virus (CaMV) 35S promoter (*35S:XGD1*), the reduced xylose content of the cell wall material was restored to the wild type level (Table 3). Transformation of *qrt* plants with the same construct had no effect on the monosaccharide compo-sition. These experiments show that the *XGD1* coding sequence

A pectin-enriched fraction from the wild type (*qrt*) and *xgd1-1* was treated with XGA hydrolase (XGH) and subjected to HPAEC and MALDI-TOF MS analysis. Identity of the peaks was determined from the masses and retention times (Zandleven et al., 2007). Similar results were obtained in two experiments with independent samples.

product from the wild type was $GalA_3Xyl$ followed by a significant formation of GalA, GalAXyl, $GalA_2Xyl$, $GalA_4$, and $GalA_5$ and a minor production of $GalA_2Xyl_2$, $GalA_2Xyl'$, and $GalA_6$. Although it cannot be excluded that XGA that is resistant to XGA hydrolase exists in *xgd1-1*, the XGA content in *xgd1-1* is clearly reduced compared with the wild type.

Analysis of T-DNA Insertion Lines in XGD1 by Immunohistochemistry

A monoclonal antibody, LM8, with specificity for XGA was raised against a highly substituted form of XGA and has previously been described (Willats et al., 2004). Immunolabeling of the wild type (*qrt*) and *xgd1-1* was used to determine if this XGA epitope was affected in *xgd1-1* (Figure 5). The LM8 XGA epitope has a highly restricted distribution in *Arabidopsis* and was only detected in roots (Figures 5A and 5B) and siliques (Figures 5C and 5D). LM8 binding was identical in these organs in *qrt* and *xgd1-1.* Our biochemical analysis indicated that XGA is abundant in leaves, and the lack of LM8 binding to this XGA may be because the XGA in leaves does not have a sufficient level of xylose substitution to be recognized by LM8. Labeling of leaves with the anti-HG mAb JIM5 and calcofluor, which stains b-linked glucans, indicated that HG levels and overall cellular anatomy were not affected in *xgd1-1.* Together with biochemical analyses, these data indicate that a less substituted form of XGA that is abundant in leaves is a likely product of XGD1 but that the highly substituted XGA epitope recognized by LM8 is not.

Complementation of the Mutant Phenotype

The identical wall phenotype in the two independent alleles *xgd1-1* and *xgd1-2* (Figure 2) strongly indicates that the lack of can complement the *xgd1* mutant phenotype. Furthermore, introduction of a construct expressing a recombinant XGD1 protein fused to a combined *c*-myc-6xHis affinity tag in its C-terminal end adding a total of 24 amino acids (*35S:XGD1-Myc-6-His*) also complemented the *xgd1* phenotype (i.e., the xylose content was again restored to the wild type level) (Table 3). By contrast, complementation was not obtained when the *xgd1-1* plants were expressing an N-terminally truncated version of the XGD1 protein lacking the first 160 amino acid residues compris-ing the signal anchor and part of the stem region (*35S:*D*N-XGD1*). The truncated version corresponds to cDNA clones with Gen-Bank accession numbers AAK83577 and AAL62020, and the lack of complementation indicates that these clones are not full length.

XGD1 Transiently Expressed in Nicotiana benthamiana Has XGA Xylosyltransferase Activity

The wall phenotype of the T-DNA mutants indicated that XGD1 is involved in XGA biosynthesis. Given that glycosyltransferase Family 47 is known to contain inverting glycosyltransferases, the indication was that XGD1 would most likely be a XGA b-1,3-xylosyltransferase. To investigate this possibility, we expressed the *35S:XGD1* and *35S:XGD1-Myc-6-His* constructs in *N. ben-thamiana* leaves by *Agrobacterium*-mediated transient ex-pression. The transient expression leads to accumulation of substantial amounts of heterologous protein as shown by im-munoblotting using anti-His-tag antibodies (see Supplemental Figure 6 online). Microsomes were prepared from leaves 4 d after infiltration and used for the glycosyltransferase assays. We tested activity using different NDP-^{14}C-sugars as donor sub-strates and heat-treated microsomes prepared from noninfiltra-ted *N. benthamiana* leaves as acceptors (Figure 6A). Microsomes expressing *35S:XGD1* showed highly increased activity trans-ferring ^{14}C-Xyl from UDP-^{14}C-Xyl to polymeric products pre-cipitated in 70% ethanol compared with control microsomes, whereas no significant change in activity was observed with UDP-^{14}C-Glc, UDP-^{14}C-Gal, or UDP-^{14}C-GlcNAc. With UDP-^{14}C-GlcA, we observed a small increase in activity compared with the control. However, the background activity from endoge-nous glycosyltransferases was very high with UDP-GlcA, and this makes it difficult to conclude whether there is any increased incorporation of GlcA in the presence of XGD1. The same is true to some extent with UDP-Gal. Thus, *XGD1* fusion protein was actively expressed in *N. benthamiana* and showed xylosyltrans-ferase activity transferring xylose onto endogenous oligosac-charides present in *N. benthamiana* microsomes. To investigate the nature of the products formed, we treated the products obtained with UDP-^{14}C-Xyl with XGA hydrolase. As shown in Figure 6B, the majority of the ethanol-insoluble ^{14}C-products that were synthesized using microsomes expressing *35S:XGD1* were released to an ethanol-soluble supernatant after treatment with XGA

hydrolase. This indicates that the ^{14}C-products syn-thesized by *35S:XGD1* were mainly XGA. ^{14}C-products synthe-sized by control microsomes also released some radioactivity into an ethanol-soluble supernatant. This may be due to endog-enous XGA xylosyltransferase activity and to a minor extent may also be due to release of unrelated ^{14}C-materials copreci-pitated with XGA but released together with XGA after hydrolase treatment.

Under the same assay condition, we also investigated whether pure oligogalacturonides with degree of polymerization of 12 to 14 could act as acceptors. Microsomes expressing *35S:XGD1* transferred ^{14}C-Xyl from UDP-^{14}C-Xyl to these acceptors, and synthesized ^{14}C-products precipitated in 70% ethanol to a much higher extent than the control (Figure 6C). Analysis of the data by two-way ANOVA shows a significant effect of adding oligoga-lacturonides ($P < 0.001$) and of XGD1 versus control ($P < 0.02$). There was no significant effect of adding oligogalacturonides to the control reactions (*t* test, $P > 0.05$). Thus, XGD1 expressed in *N. benthamiana* also showed xylosyltransferase activity onto exogenous oligogalacturonide acceptors.

XGD1 Is Located in Golgi Vesicles

An in-frame fusion of XGD1 and yellow fluorescent protein (YFP) was generated and transiently expressed in *N. benthamiana* leaves via *Agrobacterium* infiltration. Leaves expressing XGD1-YFP fusion protein accumulated the YFP signal in small, moving, oval dots (Figure 7B), while YFP, when expressed without fusion, accumulated uniformly in cytosol and in nuclei (Figure 7A). The XGD1-YFP fusion protein was coexpressed with known marker proteins. Figures 7C and 7E show confocal images of a leaf coexpressing XGD1-YFP and GFP-HDEL (an endoplasmic re-ticulum [ER] marker), respectively, and Figure 7G shows the superimposition. It is noteworthy that XGD1-YFP and green fluorescent protein (GFP)-HDEL showed distinct distribution patterns, the former showing an interspersed dot distribution and the latter showing a uniform distribution along the cell periphery with spiderweb-like meshwork, which is characteristic of ER. Figures 7D and 7F show confocal images of a leaf coexpressing XGD1-YFP and STtmd-GFP (a Golgi marker; Boevink et al., 1998), respectively, and Figure 7H shows the superimposition of the two signals, showing near-perfect coloc-alization. The signals from the two proteins moved together, providing further evidence that the proteins were colocalized. Taken together, these results demonstrate that XGD1-YFP fu-sion protein localizes in the Golgi apparatus in *N. benthamiana*.

DISCUSSION

T-DNA Insertion in XGD1 Causes a Specific Decrease in XGA Content

T-DNA insertion in the *XGD1* locus resulted in decreased cell wall xylose content (Figures 2 to 4, Table 2). Both investigated insertion lines (*xgd1-1* and *xgd1-2*) show an identical decrease in cell wall xylose (Figure 2), even though only *xgd1-1* is a true mRNA knockout line (i.e., with no detectable transcript). The T-DNA in-sertion in *xgd1-2* results in a chimeric protein that is altered in the conserved C-terminal end and predicted to be nonfunctional. Complementation with *XGD1* confirmed that the phenotype of the mutants is due to the lack of a functional *XGD1* gene.

XGA has previously been shown to be present in *Arabidop-sis*, based on digestion of pectic extracts with XGA hydrolase (Zandleven et al., 2007). Cell wall material isolated from adult leaves of *xgd1-1* and the wild type (*qrt*) was analyzed for the presence of XGA using the same procedure, and while XGA oligomers could be detected in the wild type extract, no XGA oligomers were detected in the *xgd1-1* extract. These results clearly demonstrate that XGD1 is involved in biosynthesis of XGA. An important question is whether the xylose deficiency in the *xgd1* mutants is specific for XGA or whether other xylose-containing polymers could also be affected. We focused on *xgd1-1* to establish which cell wall polymer was affected by the disruption of *XGD1* function and concluded that the xylose deficiency was attributable to altered XGA, while no other poly-mers showed decreased xylose levels. Based on immunological studies and analysis of the residue after extraction of pectin, we could not detect any decrease in the levels of the major xylose-containing polymers xylan and xyloglucan in the *xgd1-1* mutant. Furthermore, the xylose deficiency is not a general decrease in xylose, and the deficiency of xylose can be accounted for by the decrease in XGA (i.e., terminal xylose in the pectic fraction). In this context, it is important to note that the xylose deficiency varied between experiments from ;15 to ;30% of the leaf xylose. This variation is probably due partly to changes in the content of other xylose-containing polymers, such as xylan, which is abundant in tissues with more secondary walls. How-ever, the amount of XGA is also clearly variable, as evidenced by variation in Xyl:Rha ratios in pectin extracts from ;1:3 to 1:5. This level of variation is not surprising given the differences in *XGD1* expression in tissues of different age and in response to stresses (see Supplemental Figure 2 online). In conclusion, the mutant wall phenotype clearly suggests that XGD1 is specifically involved in the biosynthesis of XGA.

XGD1 Is a Member of Glycosyltransferase Family 47 and Has XGA Xylosyltransferase Activity

The backbone of XGA is composed of a-1,4-linked galacturonic acid residues and is expected to be synthesized by a retaining galacturonosyltransferase. Enzymes with HG galacturonosyl-transferase activity have been found in the GAUT subgroup of glycosyltransferase Family 8 (Sterling et al., 2006), and it is highly plausible that the backbone of XGA is synthesized by members of the GAUT group or the related GATL group. The xylose residues of XGA are b-1,3-linked and hence should be synthe-sized by an inverting glycosyltransferase. Heterologous expres-sion of XGD1 in *N. benthamiana* showed that the enzyme is capable of transferring xylose from UDP-xylose onto endog-enous acceptors in microsomes and to oligogalacturonides. The observed activity with endogenous acceptors was ;3 nmol xylose incorporated per mg protein, corresponding to ;150 pmol in each reaction. This level of activity is similar to what has been observed in other heterologous expression experiments with cell wall–related glycosyltransferases that are Type II mem-brane proteins

(Perrin et al., 1999; Faik et al., 2002; Madson et al., 2003; Egelund et al., 2006; Sterling et al., 2006). The product could be cleaved with highly specific XGA hydrolase. With oligogalacturonides the activity was consistently lower than with endogenous acceptors, indicating that pure oligogalactur-onides are not the optimal acceptors. Perhaps acceptors with some rhamnose would be better substrates and that could explain why XGA appears to be associated with RGI and not randomly distributed on HG. However, the limited availability of well-defined pectin fragments has prevented a more detailed analysis.

XGD1 belongs to glycosyltransferase Family 47, which is known to contain inverting enzymes. Among the members of the family, most have an unknown activity, but those that have been investigated in more detail do not have common sugar specificity and they do not catalyze formation of a particular linkage. Clearly, additional biochemical analysis of the XGD1 protein is necessary to determine the linkage formed by the enzyme, but the data reported here strongly indicate that XGD1 is an XGA b-1,3-xylosyltransferase. While xylosyltrans-ferase activity of XGD1 was demonstrated, it can be speculated if higher activity would be obtained with simultaneous elonga-tion of the galacturonic acid backbone, like the arabinoxylan arabinosyltransferase (Porchia et al., 2002) or the galacto-mannan galactosyltransferase (Edwards et al., 1989). However, we did not observe any increase in xylosyltransferase activity when tobacco microsomes with heterologously expressed XGD1 were coincubated with UDP-^{14}C-Xyl and UDP-GalA (data not shown).

XGD1 Is Located in Golgi Vesicles

Pectin biosynthesis, or at least the major part of it, is believed to occur in the Golgi apparatus (Scheller et al., 2007). No reports are available on the specific site of synthesis of XGA, but presumably this would also take place in the Golgi vesicles. We determined that XGD1, studied as an XGD1-YFP fusion protein, colocalized with the known Golgi marker STtmd-GFP (Boevink et al., 1998). This further supports our notion that XGD1 is involved in pectin biosynthesis. The observation that the N-terminally truncated version of XGD1 was unable to complement the mutant pheno-type is presumed to be a consequence of the missing signal an-chor and transmembrane domain. Even though this N-terminally truncated protein possibly could be active, it would not be localized in the right subcellular biosynthetic compartment. As mentioned previously, the *xgd1-2* plants, which are expected to express a chimeric protein where 30 amino acids of the C terminus are replaced by 20 or more amino acids coded by the T-DNA, display the same xylose-deficient phenotype as *xgd1-1*. These 30 amino acids, which have been substituted in *xgd1-2*, are part of a highly conserved region among all genes within glycosyltransferase Family 47 subgroup C in both *Arabidopsis* and rice (*Oryza sativa*). Therefore, it is plausible that this region is important with respect to catalytic activity. Interestingly, the C-terminally tagged protein (XGD1-myc-6-His) was able to complement the mutant phenotype and show xylosyl transferase activity in vitro, confirming that extension of the C terminus does not interfere significantly with catalytic activity or subcellular localization.

Arabidopsis Contains at Least Two Different Types of XGA

The XGA of wild-type leaves was greatly decreased in the mutant based on the biochemical measurements of sugar content and the enzymatic fingerprinting. However, we could still detect the LM8 epitope in root tips and in the septa of siliques. Interestingly, the LM8 antibody did not give rise to any labeling in mature leaves in the wild type where the *XGD1* gene is most highly expressed. The distribution in mature leaves of partially methyl-esterified HG (JIM 5 epitope) and the overall cell shape and tissue structure as visualized by calcofluor staining did not reveal any differences between the wild type and *xgd1-1*. The precise epitope of LM8 is not known, but it has previously been suggested that LM8, which has been raised against XGA isolated from pea (*Pisum sativum*) testae, binds to a highly substituted epitope of XGA possibly substituted with a disaccharide of xylose that is not susceptible to cleavage by an exopolygalac-turonase or the XGA hydrolase used in this work (Willats et al., 2004). No LM8 epitope could be detected in leaves, but the pectin fraction from *xgd1-1* still contained a significant amount of terminal xylose and 3,4-GalA. Since the remaining xylose could not be released with XGA hydrolase, we cannot be certain about the nature of the polymer that contains the xylose and 3,4-GalA. However, the most obvious interpretation is that the leaves also contain a more highly substituted XGA, which is unaffected in the *xgd1* mutant. Therefore, our results suggest the presence of at least two different types of XGA in *Arabidopsis*, a low substituted form, synthesized by XGD1, which is generally present in all green tissues and carries single xylose substitutions (Zandleven et al., 2007), and a highly substituted form, which is highly resistant to enzymatic hydrolysis. The fact that LM8 can only detect labeling in certain tissues could indicate variations in the highly substituted XGA or shielding of the epitope in leaves. The presence of two types of XGA in *Arabidopsis* suggests that one or more of the XGD1 paralogs are involved in the biosynthesis of the highly substituted XGA.

XGD1 and Paralogs in the Glycosyltransferase Family 47 Subgroup C Are All Predicted to be Membrane-Bound Glycosyltransferases

Previous annotation of XGD1 (At5g33290) predicted the protein to be soluble and without a transmembrane domain (Li et al., 2004). The original annotation was based on cDNAs that were apparently not full length. However, the longer cDNA used in this work indicates that XGD1 is a Type II membrane protein. According to the nomenclature used at http://cellwall.genomics. purdue.edu, XGD1 (At5g33290) belongs to subgroup C of CAZy GT Family 47. Nomenclature and grouping have been modified compared with what was earlier described

(Li et al., 2004). In addition to XGD1, four of the other members of subgroup C (At3g42180, At5g20260, At5g11130, and At5g25310) had also been predicted to be soluble proteins according to the original annotation (Li et al., 2004). However, by thorough analysis of the gene structure and the translated sequence of the other mem-bers of this group (see Supplemental Figure 7 and Supplemental Methods 1 online), we have been able to re-annotate these genes and suggest that they all encode membrane proteins. Further-more, all genes within this group share the same intron-exon structure according to our annotation. The relatively large intron 2 varying in size from 72 to 2409 bp, a potential alternative start codon in exon 3, and the lack of supporting cDNA sequence information is the likely explanation for the previous annotation difficulties within this group. The similarity in sequence and topology between the proteins suggests that they are all Golgi-located glycosyltransferases involved in cell wall biosynthesis. At present, there is no information about the possible function of the other members in the subgroup. Furthermore, only one of the paralogs (At5g03795, re-annotated from At5g03800) is present on the Affymetrix ATH1 microarray chip, limiting possible data mining efforts and in silico expression analysis. We have ana-lyzed insertional mutants of At3g42180 and At5g25310 and have not been able to detect any difference in monosaccharide composition of leaf cell walls (see Supplemental Figure 8 online). However, this may be due to redundancy between some of the proteins or to the activity of some proteins being restricted to special and limited conditions or cell types. For example, as mentioned above, we find it likely that one or more of the paralogs would be specifically involved in synthesizing the XGA of root tips or septa of siliques, and this would not be detected by monosaccharide composition analysis of leaf cell wall material.

Role of XGA

XGA has been reported to be abundant in reproductive tissues of many plants and has recently also been shown to be present at high levels in vegetative tissues of *Arabidopsis* (Zandleven et al., 2007). No specific function has been assigned to XGA, but the abundance of this polymer would almost certainly affect the physical properties of the pectic matrix. Thus, the calcium-dependent interactions between HG chains would be prevented from forming if the chains are substituted with xylose. How this might affect the biology of the plant is unclear. XGA is resistant to digestion by endopolygalacturonases, and this can be predicted to affect the plant. Although enzymes such as the XGA Hydrolase 1298 used in this study are capable of degrading XGA, these enzymes appear to be much less common than the endopolygalacturo-nases that are abundantly synthesized by plants themselves and by plant pathogens. Hence, the presence of substituted galacturonans can be predicted to affect development (for example, pectin degradation during fruit ripening) and the re-sponse to pathogens. In this context, it is interesting to note that *XGD1* mRNA is increased in response to several pathogens like *Botrytis cinerea*, *Phytophtora infestans*, and *Pseudomonas sy-ringae* and when syringolin and methyl-jasmonate are applied, suggesting a function of XGA in resistance to pathogen attack. Future studies will be directed at determining the biological significance of XGA.

METHODS

Plant Material

All *Arabidopsis thaliana* lines used in this work are derived from ecotype Col-0. Seed of T-DNA insertion line SAIL 1175_H04 (*xgd1-1*) and the corresponding background line (*qrt*; referred to as the wild type when in comparison with *xgd1-1*) were obtained from Syngenta. T-DNA insertion line SALK_087620 (*xgd1-2*) was obtained from the Salk institute (Alonso et al., 2003).

Plants were grown in peat at an 8-h photoperiod at 100 to 120 mmol photons m^{-2} s^{-1}, 208C, and 70% relative humidity and watered using tap water as necessary. Fertilizer was not used. Young leaves were harvested at the 10 to 12 leaf stage and adult leaves after ;12 weeks of growth. To initiate bolting and synchronize stem growth, plants were shifted to a 16-h photoperiod after 8 weeks of growth in the 8-h photoperiod. Roots for real-time RT-PCR were obtained from plants grown hydroponically (Husted et al., 2002). Roots for immunolabeling were obtained from 5-d-old seedlings grown vertically on Murashige and Skoog medium, pH 5.7, containing 1% sucrose and 0.8% bacto-agar (Difco).

Bioinformatics

Protein targeting was predicted using TargetP (Emanuelsson et al., 2000), signal peptide or signal anchor predictions were predicted using SignalP 3.0 (Bendtsen et al., 2004), transmembrane helices were predicted using TMHMM Server v. 2.0 (http://www.cbs.dtu.dk/services/TMHMM-2.0/; Sonnhammer et al., 1998), and *N*-glycosylation sites were predicted using NetNGlyc (http://www.cbs.dtu.dk/services/NetNGlyc/).

In silico expression analysis and response viewer were performed using the Genevestigator data mining tool, which is based on publicly available microarray experiments (Zimmermann et al., 2004).

Three out of the six closest homologs to XGD1 in *Arabidopsis* (At5g20260, At5g11130, At5g25310, and At3g42180) were re-annotated and aligned as described in Supplemental Methods 1 and Supplemental Figure 7 online.

Identification of Homozygous Plants

Genomic DNA was prepared as described by Edwards et al. (1991). *xgd1-1* homozygous plants were identified by PCR using primers suggested by Syngenta (gene-specific primers 59-GGGTTTAGCTGGGACGATTCAA-39 and 59-CCGACCTAACGTGGACGTAT-39, insert-specific primer 59-TAG-CATCTGAATGTCATAACCAAT-39). For *xgd1-2*, the T-DNA insert was reported to be located in the last exon of *XGD1* ;500 bp upstream from the stop codon according to the SIGnAL T-DNA Express *Arabidopsis* Gene Mapping Tool (http://signal.salk.edu/cgi-bin/tdnaexpress; Alonso et al., 2003). However, when

potential T-DNA mutant plants were screened by PCR using primers suggested by the Salk Institute (forward gene-specific primer 59-TCAAGACGAATGAGTCGGAG-39 and reverse gene-specific primer 59-CCAAATTTTGTTTGGCTTGAA-39, insert-specific primer, LBa1, 59-TGGTTCACGTAGTGGGCCATCG-39; Figure 1), an unex-pected large insert product was obtained using the forward gene-specific primer for *xgd1-2* in combination with the T-DNA insert-specific primer LBa1. This indicated that the true location of T-DNA insertion was in fact much further downstream in the *XGD1* gene than initially identified. This hypothesis was verified by sequencing of the PCR product generated by the forward primer and LBa1 using sequencing primer 59-CATTACCATT-CAGTGATGTGC-39. To be able to deduce the protein sequence of xgd1-2 (see Supplemental Figure 1 online), the 39 end of the *xgd1-2* mRNA was amplified by a nested PCR approach. First round of PCR was preformed with the primers 59-CAAGTAAAAAAATTGTTATCAGGAAAAG-39 (span-ning exon 1 and exon 2) and 59-TTTTTTTTTTTTTTTTTTTTTTTTTTTTTTV-39 (V symbolizing C/A/G) and using *xgd1-2* cDNA (prepared as below) as template. A successive nested PCR was then preformed using the primers 59-CGCCTTTCATCAGAGTCAC-39 (spanning exon 2 and exon 3) and 59-TTTTTTTTTTTTTTTTTTTTTTTTTTTTTV-39. The resulting PCR product from the nested PCR was subsequently sequenced using the primers 59-AGATCGACCCGAGAATGC-39 (verifying the exon 3–exon 4 junction) and 59-TTGTCTGTGTCCGAGTGG-39 (sequencing the furthest 39 part of the mRNA).

Gene Expression Analysis

Total RNA was isolated from roots, young leaves, adult leaves, stems, and flowers using the RNeasy plant mini kit (Qiagen). cDNA was prepared from 1 mg of total RNA using the iScript cDNA synthesis Kit (Bio-Rad) in a total volume of 25 mL. One microliter was used for real-time RT-PCR amplification of *XGD1* with gene-specific primers (59-CCATGACTGG-CACCAGACGT-39 and 59-TATCCTAGAAACAGGGATTTGTATGG-39) us-ing an ICycler Instrument (Bio-Rad) with the iQ SYBR Green Supermix kit for PCR (Bio-Rad) according to the manufacturer's instructions. The reactions were incubated at 968C for 3 min to activate the hot start recombinant Taq DNA polymerase, followed by 50 cycles of 1 min at 968C, 1 min at 608C, and 1 min at 728C. The specificity of the PCR amplification was checked with a heat dissociation protocol (from 65 to 958C) following the final cycle of the PCR. The results obtained for the different samples analyzed were standardized to the polyubiquitin 10 RT-PCR product level using the primers 59-GGCCTTGTATAATCCCTGAT-GAATAAG-39 and 59-AAAGAGATAACAGGAACGGAAACATAGT-39.

Preparation and Chemical Analysis of Cell Wall Material

Cell wall material and subsequent RGI/XGA extraction was prepared from leaves as destarched alcohol-insoluble residue as previously described (Harholt et al., 2006). For RGI/XGA extraction and XGA endohydrolase digestion, the cell wall material was further phenol:acetic acid:water (2:1:1 v/v) treated as previously described (Harholt et al., 2006). Mono-saccharide composition analysis was performed on alcohol-insoluble residue and RGI isolated from leaves using the high-performance anion exchange chromatography method previously described (Øbro et al., 2004). For glycosidic linkage analysis, isolated RGI was methylated using sodium hydroxide and methyl iodide in dimethyl sulfoxide (Ciucanu and Kerek, 1984). For linkage analysis of carboxyl groups of pectin-derived GalA residues, the methylated pectin fraction was subsequently reduced with lithium triethylborodeuteride (Superdeuteride; Sigma-Aldrich) (York et al., 1985). Partially methylated alditol acetates were generated as previously described (Harholt et al., 2006).

Statistical analyses were always based on data obtained with multiple individual wall preparations, and the *n* values given in figure legends relate to the number of biological replicates. For the monosaccharide composition data, the within sample reproducibility was very high com-pared with the biological variation.

Comparative Immunomicrodot Assay Analysis

Polymers were sequentially extracted from homogenized plant material using *trans*-1,2-diaminocyclohexane-*N*, *N*, *N*9, *N*9-tetraacetic acid, NaOH, and cadoxen (1,2-diaminoethane and cadmium oxide). These three solvents are known to solubilize pectins, noncellulosic polysac-charides, and cellulose, respectively (Fry, 2000). Supernatants from the extractions were spotted onto nitrocellulose membrane using a micro-array robot (Microgrid II; Genomic Solutions). Arrays were probed with monoclonal antibodies with specificity for galactan (LM5; Jones et al., 1997), arabinan (LM6; Willats et al., 1998), xyloglucan (CCRCM1; Puhlmann et al., 1994), and xylan (LM11; McCartney et al., 2005). Spot signals were scanned and converted to 16-bit grayscale TIFFs and then quantified by means of microarray analysis software (ImaGene 4.0; BioDiscovery). Fold changes in antibody binding were calculated from background-corrected spot signals.

Extraction and Analysis of XGA by HPAEC-PAD and MALDI-TOF MS

Treatment with XGA hydrolase was performed as described by Zandleven et al. (2007). Alcohol-insoluble residue was extracted with phenol:acetic acid:water, saponified in 0.1 M sodium hydroxide for 24 h at 48C, and subsequently neutralized with 0.1 M acetic acid. After neutralization, samples were dialyzed overnight against MilliQ water and freeze-dried. A pectin-enriched fraction was extracted at 48C using 5 mM EDTA and 50 mM NaOH (Voragen et al., 1983). The pectin-enriched fraction and remaining residue was dialyzed overnight against MilliQ water followed by dialysis overnight against 50 mM NaOAc, pH 3.5, prior to treatment by XGH. XGA hydrolase from *Aspergillus tubingensis* was expressed hetero-logously in *Aspergillus niger* and purified as described (Zandleven et al., 2007). Pectin-enriched fraction and residue from the wild type and *xgd1-1* was subjected to digestion for 20 h at 308C with 0.35 mg/mL of XGA hydrolase in 50 mM NaOAc, pH 3.5, and the degradation products were analyzed by HPAEC-PAD and MALDI-TOF MS as previously described (Zandleven et al., 2007).

Immunolabeling and Microscopy

Leaf material and siliques from 4-week-old *xgd1-1* and *qrt* plants were placed in fixative (2% paraformaldehyde, 2.5% glutaraldehyde, and 0.1 M phosphate buffer, pH 7) and placed under vacuum for 30 min. The plant material was then left in fixative overnight at 48C and washed twice in 0.1 M phosphate buffer, pH 7.0, for 30 min each time at 48C. Samples were dehydrated in an ethanol series (30, 50, 70, 80, 90, and 100%) for 20 min each and then transferred to LR White resin (Hard Grade Acrylic Resin; London Resin Company) at 48C for 24 h with two changes to allow the resin to infiltrate the tissue. The plant material was then placed in gelatin capsules and filled with LR White resin and polymerized at 608C for 24 h. Transverse sections of leaf and silique material for both

xgd1-1 and *qrt* were cut at a thickness of 3 mm with glass knives on a microtome (LKB Bromma 2218 Historange Microtome) and placed on diagnostic microscope slides (Erie Scientific) that were coated in Vectorbond reagent (SP-1800; Vector Laboratories). Resin-embedded sections of siliques and leaves and 5-d-old root tips from *xgd1-1* and *qrt* plants for surface labeling were blocked for 1 h in 5% milk powder in PBS and then incubated with 10-fold dilutions of LM8 epitope specific for XGA. In addition, leaf resin-embedded sections were incubated with 10-fold dilution of JIM5 antibody for partially methylesterified HG. After washing the sections, the surface-labeled roots were incubated with 100-fold dilution of fluorescein isothiocyanate (Sigma-Aldrich) conjugated secondary antibody, and leaf sections were counterstained for 5 min with Calcofluor White M2R fluorochrome (fluorescent brightener 28; Sigma-Aldrich; 20 mM in phosphate buffer, pH 8) to detect the presence of cellulose. After washing with PBS, the sections were mounted in a glycerol/PBS based antifade solution (Citifluor AF1; Agar Scientific) and observed on an epifluorescence microscope (Axioplan; Zeiss).

Transformation of Plants with 35S:XGD1 Constructs

All constructs were generated on the basis of the *XGD1*-cDNA clone MPIZp2001I033Q2 (RZPD Deutsches Ressourcenzentrum fu¨r Genom-forschung, Berlin, Germany) and by the use of Phusion polymerase (Finnzymes). The *XGD1* coding region was amplified using forward primer 59-GTCCGGAGCTCATGGCTGCTCCAAGATC-39 (*Sac*I underlined) and reverse primer 59-GACATGCATGCCTATGTACCAAGCCTAAGATTAAG-39 (*Sph*I underlined). Alternatively, At5g33290 has been annotated to en-code a soluble protein that is 160 amino acids shorter than the N terminus compared with the above annotation. This version of the gene was amplified using forward primer 59-GTCCGGAGCTCATGAATCGTTT-TAAGGTGTG-39 together with the same reverse primer as above. The PCR products were cloned as a *Sac*I/*Sph*I fragment under control of the CaMV 35S promoter and terminator in pPS48 (Kay et al., 1987), resulting in pJJ28 and pJJ30, respectively. A fusion protein was generated by adding a tag to the C-terminal end of the XGD1 protein. This construct was generated by inserting the *c*-myc-6xHis cassette from the pPICZaA plasmid (Invitrogen) into pPS48 as a *Sac*I/*Sph*I fragment. This fragment was amplified using the following primers: 59-GTCCGGAGCTCGC-GGAACAAAAACTCATCTCAGAAG-39 (*Sac*I underlined) and 59-GAC-ATGCATGCGCAAATGGCATTCTGACATCC-39 (*Sph*I underlined). The complete *XGD1* coding region without stop codon was inserted as a *Sac*I/*Sac*I fragment generated by the forward primer described above and the reverse primer 59-GTCCGGAGCTCTGTACCAAGCCTAAGAT-TAAG-39 (*Sac*I underlined), resulting in pJJ29. Insert and vector-insert junctions were sequenced, and subsequently the *Xba*I fragment of pJJ28, pJJ29, and pJJ30 containing the CaMV 35S promoter, insert, and the CaMV 35S terminator was transferred to pPZP221 (Hajdukiewicz et al., 1994), resulting in p35S:XGD1, p35S:XGD1-Myc-6-His, and p35S:DN-XGD1, respectively. *qrt* and *xgd1-1* plants were transformed with empty pPZP221 vector or with the vectors containing the different *35S:XGD1*-versions by *Agrobacterium tumefaciens*–mediated transformation using the strain C58C1 pGV3850 and the floral dip method (Clough and Bent, 1998). Seeds were germinated for 2 weeks on Murashige and Skoog medium containing 100 mg/mL gentamycin sulfate, and surviving seed-lings were subsequently transferred to soil and grown as described above. After 8 weeks on soil, full-grown rosette leaves were harvested and used to prepare total cell wall alcohol-insoluble residue for determi-nation of monosaccharide composition.

Fluorescent Protein Fusion and Subcellular Localization

The full-length *XGD1* was amplified from the plasmid pJJ29 using the following primers: NT01, 59-GGCTTAAUATGGCTGCTCCAAGATCAAG-39, and NT02, 59-GGTTTAAUCCTGTACCAAGCCTAAGATTAAGTC-39, in which the underlined oligonucleotides were engineered to provide USER cloning sites (Nour-Eldin et al., 2006). The fragments were inserted into the unique USER site in pCAMBIA330035SuYFP in frame with the downstream YFP (Bernal et al., 2007). The previously described con-structs containing the in-frame fusions STtmd-GFP and GFP-HDEL were used as markers for Golgi apparatus and ER, respectively (Boevink et al., 1996, 1998). *Agrobacterium* C58C1 pGV3850 was transformed with each construct by electroporation and was selected for resistance against kanamycin (50 mg/mL). For transient transformation of *Nicotiana ben-thamiana*, the bacteria were grown over night in Luria-Bertani (LB) medium containing 10 mM MES and 20 mM acetosyringone. The bacterial cells were harvested by centrifugation and resuspended in a buffer containing 10 mM MES, 10 mM $MgCl_2$, and 100 mM acetosyringone (OD_{600} ¼ 0.05) and allowed to stand at room temperature for 2 to 3 h. Leaves of the wild-type *N. benthamiana* (6 weeks old, grown in green-house at 288C/day and 188C/night with 16 h photoperiod) were infiltrated with the bacterial cell suspensions using 2.5-mL syringes. Observations of sections of leaves were performed 24 to 48 h after infiltration. The confocal laser scanning microscope (TCS SP2; Leica Microsystems) was used to sequentially monitor GFP and YFP signals. The excitation and detection wavelengths for GFP and YFP were as follows: 488 and 514 nm for excitation, and 495 to 510 nm and 550 to 593 nm for detection, respectively.

Heterologous Expression of XGD1 and Assay for XGA Xylosyltransferase Activity

Leaves from 3-week-old wild-type *N. benthamiana* were used for *Agrobacterium*-mediated transient expression of two versions of *XGD1* constructs (*35S:XGD1* and *35S:XGD1-Myc-6-His*). To facilitate high expression of recombinant protein, strains carrying the *XGD1* constructs were coinfiltrated with a strain carrying p19, encoding p19 protein, a viral protein specifically inhibiting posttranscriptional gene silencing by the plant (Voinnet et al., 2003). *Agrobacterium* C58C1 pGV3850 strains carrying the plasmids were grown overnight in LB medium containing appropriate antibiotics (*p35S:XGD1* and *p35S:XGD1-Myc-6-His*: 100 mg/mL rifampicillin and 75 mg/mL spectomycine; p19: 100 mg/mL rifampi-cillin, 50 mg/mL kanamycin, 5 mg/mL tetracycline). The bacterial cells were suspended in a buffer as described above except that the concen-tration was higher (OD_{600} ¼ 2.0). Prior to infiltration, the bacterial sus-pensions were diluted or combined as follows: for control, 1/4 (v/v) of the strain carrying p19 in a solution of OD_{600} ¼ 2.0 and 3/4 (v/v) buffer was combined; for XGD1 expression, 1/4 (v/v) of the strain carrying p19 and 1/4 (v/v) of the strain carrying either *p35S:XGD1* or *p35S:XGD1-Myc-6-His*, all strains in a solution of OD_{600} ¼ 2.0, and 1/2 (v/v) buffer were combined. Four days after infiltration, the leaves were harvested, and microsomes were prepared according to the method described by Orfila et al. (2005) with some modifications. The leaves were extracted in 50 mM potassium phosphate, pH 6.0, 0.4 M sucrose, 100 mM sodium ascorbate, 1 mM PMSF, and protein inhibitor cocktail (25 mL/g fresh weight com-plete tablets; Roche Applied Sciences). After the first centrifugation at 1000*g* for 10 min, the supernatant was centrifuged at 100,000*g* for 1 h. Sedimented microsomes were suspended in 50 mM potassium phos-phate, pH 8.0, 1 mM EDTA, 1 mM DTT, and 10% (v/v) glycerol to a protein concentration of ;10 mg/mL.

For xylosyltransferase assay, the microsomes were first treated for 5 min with 0.3% (v/v) Triton X-100. Then, 10 mL of the Triton X-100– solubilized microsomes were incubated in 40 mM potassium phosphate, pH 8.0, 10 mM $MnCl_2$, 100 mM (370 Bq) UDP-^{14}C-xylose (or other UDP-^{14}C-sugar as indicated in

the figure legends) in the presence of acceptor, which was either 10 mL microsomes from noninfiltrated *N. benthamiana* pretreated at 908C for 20 min or oligogalacturonide mixture of DP5-10 and DP12-14. Preparation of oligogalacturonides has been described previously (van Alebeek et al., 2000). After incubation at 288C for 4 to 16 h, polysaccharide materials were precipitated in cold 70% (v/v) ethanol in the presence of 0.1 mg dextran as a carrier, and the samples were left at 3208C for 30 min prior to centrifugation at 13,000*g* for 30 min. The pellet was washed three times with prechilled 70% (v/v) ethanol and scintillation counted or further treated with XGA hydrolase.

For XGA hydrolase treatment, the pellet was dissolved in 50 mL of 50 mM sodium acetate, pH 3.5, and 0.02% (v/v) NaN_3. XGA hydrolase (35 ng protein) was added, and the samples were incubated for 16 h at 288C. Prechilled ethanol was added to 70% (v/v), and the samples were left at 3208C for 30 min prior to centrifugation at 13,000*g* for 30 min. Radioac-tivity released to the supernatant and remaining in the pellet was analyzed by scintillation counting.

UDP-^{14}C-sugars were obtained from Perkin-Elmer NEN and had the following specific activities: UDP-^{14}C-GlcA, 6.6711 GBq/mmol; UDP-^{14}C-Gal, 9.5 GBq/mmol; UDP-^{14}C-Xyl, 5.6166 GBq/mmol; UDP-^{14}C-Glc, 11.174 GBq/mmol; UDP-^{14}C-GlcNAc, 10.656 GBq/mmol.

Accession Numbers

Sequence data from this article can be found in the Arabidopsis Genome Initiative or GenBank/EMBL databases under the following accession numbers: At5g33290 (Arabidopsis Genome Initiative annotation for *XGD1*), BX831739 (full-length cDNA clone for *XGD1*), and AAK83577 and AAL62020 (partial cDNA clones for *XGD1*).

Supplemental Data

The following materials are available in the online version of this article.

Supplemental Figure 1. Multiple Protein Sequence Alignment of C Termini of CAZy Glycosyltransferase Family 47 Subgroup C and xgd1-2.

Supplemental Figure 2. Response of *XGD1* Transcript Levels to Different Treatments.

Supplemental Figure 3. Typical Chromatograms for Monosaccha-ride Composition Analysis of Cell Wall Material.

Supplemental Figure 4. Typical Chromatograms for Monosaccha-ride Composition Analysis in Extracted Pectin.

Supplemental Figure 5. Typical Chromatograms for Monosaccha-ride Composition and Glycosidic Linkage Analysis of RGI/XGA.

Supplemental Figure 6. Immunoblotting of Heterologously Expressed XGD1.

Supplemental Figure 7. Reannotation of CAZy Glycosyltransferase Family 47 Subgroup C.

Supplemental Figure 8. Monosaccharide Composition Analysis of Cell Wall Material from Insertional Mutants in Homologs of *XGD1*.

Supplemental Methods 1. Reannotation of CAZy Glycosyltransfer-ase Family 47 Subgroup C.

Supplemental Data Set 1. Text File Corresponding to Alignment in Supplemental Figure 7.

ACKNOWLEDGMENTS

Syngenta and the Salk Institute are thanked for providing the *xgd1-1* and *xgd1-2* mutant seeds, respectively. Chris Hawes (Oxford Brookes University) is thanked for the clones for STtmd-GFP and GFP-HDEL. This work was supported by the Danish Natural Science Research Council, the Danish Research Council for Technology and Production Sciences, the Danish National Research Foundation, The 6th Frame-work Programme of the European Union (Contracts MRTN-CT-2004-512265 'WallNet' and MIF1-CT-2005-021313 'GLYTRANS'), and by the Director, Office of Science, Office of Biological and Environmental Research of the U.S. Department of Energy under Contract DE-AC02-05CH11231.

REFERENCES

Alonso, J.M., et al. (2003). Genome-wide insertional mutagenesis of *Arabidopsis thaliana.* Science 301: 653–657.

Bendtsen, J.D., Nielsen, H., Heijne, G., and Brunak, S. (2004). Improved prediction of signal peptides: SignalP 3.0. J. Mol. Biol. 340: 783–795.

Bernal, A.J., Jensen, J.K., Harholt, J., Sorensen, S., Moller, I., Blaukopf, C., Johansen, B., de Lotto, R., Pauly, M., Scheller, H.V., and Willats, W.G. (2007). Disruption of ATCSLD5 results in reduced growth, reduced xylan and homogalacturonan synthase activity and altered xylan occurrence in Arabidopsis. Plant J. 52: 791–802.

Boevink, P., Oparka, K., Santa Cruz, S., Martin, B., Betteridge, A., and Hawes, C. (1998). Stacks on tracks: The plant Golgi apparatus traffics on an actin/ER network. Plant J. 15: 441–447.

Boevink, P., Santa Cruz, S., Hawes, C., Harris, N., and Oparka, K.J. (1996). Virus-mediated delivery of the green fluorescent protein to the endoplasmic reticulum of plant cells. Plant J. 10: 935–941.

Bouton, S., Leboeuf, E., Mouille, G., Leydecker, M.T., Talbotec, J., Granier, F., Lahaye, M., Hofte, H., and Truong, H.N. (2002). *QUASIMODO1* encodes a putative membrane-bound glycosyltrans-ferase required for normal pectin synthesis and cell adhesion in Arabidopsis. Plant Cell 14: 2577–2590.

Brown, D.M., Zeef, L.A., Ellis, J., Goodacre, R., and Turner, S.R. (2005). Identification of novel genes in Arabidopsis involved in sec-ondary cell wall formation using expression profiling and reverse genetics. Plant Cell 17: 2281–2295.

Ciucanu, I., and Kerek, F. (1984). A simple and rapid method for the permethylation of carbohydrates. Carbohydr. Res. 131: 209–217.

Clough, S.J., and Bent, A.F. (1998). Floral dip: A simplified method for *Agrobacterium*-mediated transformation of *Arabidopsis thaliana.* Plant J. 16: 735–743.

Coutinho, P.M., and Henrissat, B. (1999). Carbohydrate-active en-zymes: An integrated database approach. In Recent Advances in Carbohydrate Bioengineering, H.J. Gilbert, G. Davis, B. Henrissat, and B. Svensson, eds (Cambridge, UK: The Royal Society of Chemistry), pp 3–12.

Edwards, K., Johnstone, C., and Thompson, C. (1991). A simple and rapid method for the preparation of plant genomic DNA for PCR analysis. Nucleic Acids Res. 19: 1349.

Edwards, M., Bulpin, P.V., Dea, I.C.M., and Reid, J.S.G. (1989). Bio-synthesis of legume-seed galactomannans in vitro. Planta 178: 41–51.

Egelund, J., Petersen, B.L., Motawia, M.S., Damager, I., Faik, A., Olsen, C.E., Ishii, T., Clausen, H., Ulvskov, P., and Geshi, N. (2006). *Arabidopsis thaliana RGXT1* and *RGXT2* encode Golgi-localized (1,3)-a-D-xylosyltransferases involved in the synthesis of pectic rhamno-galacturonan-II. Plant Cell 18: 2593–2607.

Emanuelsson, O., Nielsen, H., Brunak, S., and von Heijne, G. (2000). Predicting subcellular localization of proteins based on their N-terminal amino acid sequence. J. Mol. Biol. 300: 1005–1016.

Faik, A., Price, N.J., Raikhel, N.V., and Keegstra, K. (2002). An *Arabidopsis* gene encoding an a-xylosyltransferase involved in xylo-glucan biosynthesis. Proc. Natl. Acad. Sci. USA 99: 7797–7802.

Francis, K.E., Lam, S.Y., and Copenhaver, G.P. (2006). Separation of Arabidopsis pollen tetrads is regulated by QUARTET1, a pectin methylesterase gene. Plant Physiol. 142: 1004–1013.

Fry, S. (2000). The Growing Plant Cell Wall: Chemical and Metabolic Analysis. (Caldwell, NJ: Blackburn Press).

Hajdukiewicz, P., Svab, Z., and Maliga, P. (1994). The small, versatile pPZP family of Agrobacterium binary vectors for plant transformation. Plant Mol. Biol. 25: 989–994.

Harholt, J., Jensen, J.K., Sørensen, S.O., Orfila, C., Pauly, M., and Scheller, H.V. (2006). ARABINAN DEFICIENT 1 is a putative arabinosyltransferase involved in biosynthesis of pectic arabinan in Arabi-dopsis. Plant Physiol. 140: 49–58.

Husted, S., Mattsson, M., Mo¨llers, C., Wallbraun, M., and Schjørring, J.K. (2002). Photorespiratory $NH_4^þ$ production in leaves of wild-type and glutamine synthetase 2 antisense oilseed rape. Plant Physiol. 130: 989–998.

Ishii, T., and Matsunaga, T. (2001). Pectic polysaccharide rhamnoga-lacturonan II is covalently linked to homogalacturonan. Phytochem-istry 57: 969–974.

Iwai, H., Hokura, A., Oishi, M., Chida, H., Ishii, T., Sakai, S., and Satoh, S. (2006). The gene responsible for borate cross-linking of pectin Rhamnogalacturonan-II is required for plant reproductive tissue devel-opment and fertilization. Proc. Natl. Acad. Sci. USA 103: 16592–16597.

Iwai, H., Masaoka, N., Ishii, T., and Satoh, S. (2002). A pectin glucuronyltransferase gene is essential for intercellular attachment in the plant meristem. Proc. Natl. Acad. Sci. USA 99: 16319–16324.

Jones, L., Seymour, G.B., and Knox, J.P. (1997). Localization of pectic galactan in tomato cell walls using a monoclonal antibody specific to (1-4)-b-D-Galactan. Plant Physiol. 113: 1405–1412.

Kay, R., Shan, A., Daly, M., and McPherson, J. (1987). Duplication of CaMV 35S promoter sequences creates a strong enhancer for plant genes. Science 236: 1299–1302.

Li, X., Cordero, I., Caplan, J., Molhoj, M., and Reiter, W.D. (2004). Molecular analysis of 10 ciding regions from Arabidopsis that are homologous to the MUR3 xyloglucan galactosyltransferase. Plant Physiol. 134: 940–950.

Madson, M., Dunand, C., Li, X., Verma, R., Vanzin, G.F., Caplan, J., Shoue, D.A., Carpita, N.C., and Reiter, W.D. (2003). The MUR3 gene of Arabidopsis encodes a xyloglucan galactosyltransferase that is evolutionarily related to animal exostosins. Plant Cell 15: 1662–1670.

Matsunaga, T., Ishii, T., Matsumoto, S., Higuchi, M., Darvill, A., Albersheim, P., and O'Neill, M.A. (2004). Occurrence of the primary cell wall polysaccharide rhamnogalacturonan II in pteridophytes, lycophytes, and bryophytes. Implications for the evolution of vascular plants. Plant Physiol. 134: 339–351.

McCartney, L., Marcus, S.E., and Knox, J.P. (2005). Monoclonal antibodies to plant cell wall xylans and arabinoxylans. J. Histochem. Cytochem. 53: 543–546.

Mohnen, D. (1999). Biosynthesis of pectins and galactomannans. In Comprehensive Natural Products Chemistry, Carbohydrates and Their Derivatives Including Tannins, Cellulose, and Related Lignins, Vol. 3, D. Barton, K. Nakanishi, O. Meth-Cohn, and B.M. Pinto, eds (Oxford, UK: Elsevier), pp. 497–527.

Nakamura, A., Furuta, H., Maeda, H., Takao, T., and Nagamatsu, Y. (2002). Structural studies by stepwise enzymatic degradation of the main backbone of soybean soluble polysaccharides consisting of galacturonan and rhamnogalacturonan. Biosci. Biotechnol. Biochem. 66: 1301–1313.

Nour-Eldin, H.H., Hansen, B.G., Nørholm, M.H.H., Jensen, J.K., and Halkier, B.A. (2006). Advancing uracil-excision based cloning to-wards an ideal technique for cloning PCR fragments. Nucleic Acids Res. 34: e122.

Øbro, J., Harholt, J., Scheller, H.V., and Orfila, C. (2004). Rhamno-galacturonan I in *Solanum tuberosum* tubers contains complex arabinogalactan structures. Phytochemistry 65: 1429–1438.

O'Neill, M.A., Ishii, T., Albersheim, P., and Darvill, A.G. (2004). Rhamnogalacturonan II: Structure and function of a borate cross-linked cell wall pectic polysaccharide. Annu. Rev. Plant Biol. 55: 109–139.

Orfila, C., Sørensen, S.O., Harholt, J., Geshi, N., Crombie, H., Truong, H.-N., Reid, J.S.G., Knox, J.P., and Scheller, H.V. (2005). *QUASIMODO1* is expressed in vascular tissue of *Arabidopsis thaliana* inflorescence stems, and affects homogalacturonan and xylan bio-synthesis. Planta 222: 613–622.

Perrin, R.M., DeRocher, A.E., Bar-Peled, M., Zeng, W., Norambuena, L., Orellana, A., Raikhel, N.V., and Keegstra, K. (1999). Xyloglucan fucosyltransferase, an enzyme involved in plant cell wall biosynthesis. Science 284: 1976–1979.

Porchia, A.C., Sørensen, S.O., and Scheller, H.V. (2002). Arabinoxylan biosynthesis in wheat. Characterization of arabinosyltransferase ac-tivity in Golgi membranes. Plant Physiol. 130: 432–441.

Puhlmann, J., Bucheli, E., Swain, M.J., Dunning, N., Albersheim, P., Darvill, A.G., and Hahn, M.G. (1994). Generation of monoclonal antibodies against plant cell-wall polysaccharides. I. Characterization of a monoclonal antibody to a terminal a-(1/2)-linked fucosyl-containing epitope. Plant

Physiol. 104: 699–710.

Scheller, H., Jensen, J.K., Sørensen, S.O., Harholt, J., and Geshi, N. (2007). Biosynthesis of pectin. Physiol. Plant. 129: 283–295.

Sonnhammer, E.L., von Heijne, G., and Krogh, A. (1998). A hidden Markov model for predicting transmembrane helices in protein se-quences. Proc. Int. Conf. Intell. Syst. Mol. Biol. 6: 175–182.

Sterling, J.D., Atmodjo, M.A., Inwood, S.E., Kolli, V.S.K., Quigley, H.F., Hahn, M.G., and Mohnen, D. (2006). Functional identification of an Arabidopsis pectin biosynthetic homogalacturonan galacturono-syltransferase. Proc. Natl. Acad. Sci. USA 103: 5236–5241.

van Alebeek, G.-J.W.M., Zabotina, O., Beldman, G., Schols, H.A., and Voragen, A.G.J. (2000). Esterification and glycosylation of oligogalacturonides: Examination of the reaction products using MALDI-TOF MS and HPAEC. Carbohydr. Polym. 43: 39–46.

Voinnet, O., Rivas, S., Mestre, P., and Baulcombe, D. (2003). An enhanced transient expression system in plans based on suppression of gene silencing by the p19 protein of tomato bushy stunt virus. Plant J. 33: 949–956.

Voragen, A.G.J., Timmers, J.P.J., Linssen, J.P.H., Schols, H.A., and Pilnik, W. (1983). Methods of analysis for cell-wall polysaccha-rides of fruits and vegetables. Z. Lebensm. Unters. Forsch. 177: 251–256.

Willats, W.G.T., Marcus, S.E., and Knox, J.P. (1998). Generation of monoclonal antibody specific to (1-5)-a-L-arabinan. Carbohydr. Res. 308: 149–152.

Willats, W.G.T., McCartney, L., Mackie, W., and Knox, J.P. (2001). Pectin: Cell biology and prospects for functional analysis. Plant Mol. Biol. 47: 9–27.

Willats, W.G.T., et al. (2004). A xylogalacturonan epitope is specifically associated with plant cell detachment. Planta 218: 673–681.

York, W.S., Darvill, A.G., McNeil, T., Stevenson, T.T., and Albersheim, P. (1985). Isolation and characterization of plant cell walls and cell wall components. Methods Enzymol. 118: 3–40.

Zandleven, J.S., Beldman, G., Bosveld, M., Schols, H.A., and Voragen, A.G.J. (2006). Enzymatic degradation studies of xylogalac-turonans from apple and potato, using xylogalacturonan hydrolase. Carbohydr. Polym. 65: 495–503.

Zandleven, J., Sørensen, S.O., Harholt, J., Beldman, G., Schols, H.A., Scheller, H.V., and Voragen, A.G.J. (2007). XGA exists in cell walls from various tissues of *Arabidopsis thaliana.* Phytochemistry 68: 1219–1226.

Zhong, R., Pena, M.J., Zhou, G.K., Nairn, C.J., Wood-Jones, A., Richardson, E.A., Morrison, W.H., Darvill, A.G., York, W.S., and Ye, Z.H. (2005). Arabidopsis *fragile fiber8*, which encodes a putative glucuronyltransferase, is essential for normal secondary wall syn-thesis. Plant Cell 17: 3390–3408.

Zimmermann, P., Hirsch-Hoffmann, M., Hennig, L., and Gruissem, W. (2004). GENEVESTIGATOR. Arabidopsis microarray database and analysis toolbox. Plant Physiol. 136: 2621–2632.

Figure 1. Schematic Structure and Transcript Analysis of the At2g35100 Locus.

Table 1. Relative Transcript Level of the *XGD1* Locus

Tissue	Wild Type	Genevestigator	*xgd1-1*	*xgd1-2*
Stems	0.08	0.15	<0.001	ND
Adult leaves	1.00	1.00	<0.001	1.03
Juvenile leaves	0.48	0.57	<0.001	ND
Roots	0.05	0.55	<0.001	ND

The data were derived from the means of real-time RT-PCR experiments with duplicate independent samples. The results obtained for the differ-ent tissues were normalized to *POLYUBIQUITIN 10* expression and ex-pressed relative to adult wild-type leaves. Data from publicly available array experiments were analyzed by Genevestigator (Zimmermann et al., 2004) and shown for comparison. ND, not determined.

Figure 2. Monosaccharide Composition of Cell Walls of the Wild Type and *xgd1* Mutants.

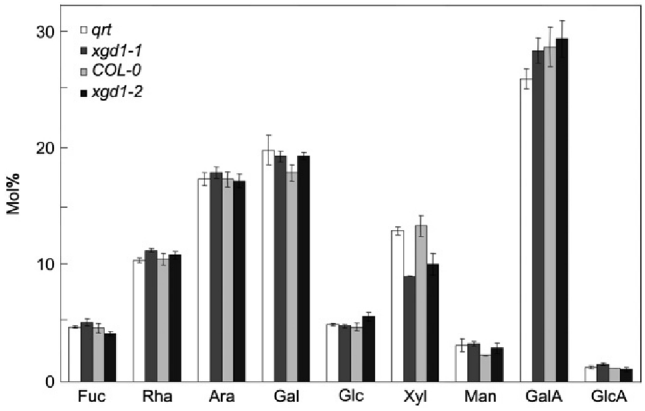

Figure 3. Monosaccharide Composition in Extracted Pectin and Resi-due from the Wild Type and *xgd1-1* Mutant.

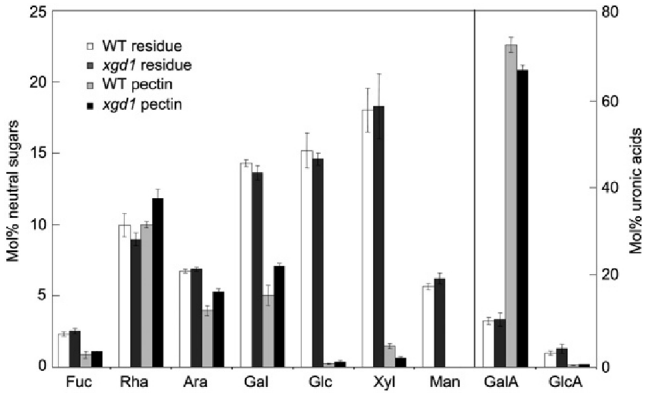

Table 2. Monosaccharide Composition and Linkage Analysis of RGI/XGA Isolated from Adult Leaves from the Wild Type (*qrt*) and *xgd1-1*

	qrt	*xgd1-1*

Monosaccharide Composition (mol %)		
Fuc	2.7	3.2
Rha	19.2	20.9
Ara	26.1	27.5
Gal	9.2	15.0
Glc	Trace	Trace
Xyl	3.8	1.2
GalA	37.9	30.8
GlcA	1.0	1.4
Linkage Analysis (mol %)		
2-Rha	15.6	12.9
2,4-Rha	8.4	10.5
t-Xyl	4.6	1.1
t-Gal	7.4	9.0
4-Gal	8.9	12.8
3-Gal	3.4	3.1
6-Gal	3.4	2.4
3,6-Gal	5.4	4.3
3,4-Gal	1.5	1.2
4,6-Gal	0.7	1.0
t-Ara*f*	4.9	5.9
5-Ara*f*	17.7	18.6
2,5-Ara*f*	3.0	3.4
2,3,5-Ara*f*	2.7	4.1
t-Fuc	0.7	0.8
4-GalA	33.4	28.4
3,4-GalA	4.5	2.4

A reduction in t-Xyl in *xgd1-1* could be observed in both the monosac-charide composition and in the linkage analysis, and a reduction in 3,4-GalA was also observed. The neutral sugars and uronic acids were determined in separate analyses, and the combined mol % of 4-GalA and 3,4-GalA was calculated according to the monosaccharide com-position (top). No other sugars or sugar derivates than those mentioned in the table could be detected. Similar results were obtained in two independent experiments.

Table 3. Complementation of the *xgd1* Mutant Phenotype

Plant Genotype	Relative Xylose Content (Wild Type ¼ 100)
qrt þ *pPZP221*	100 6 2a
qrt þ *p35S:XGD1*	104 6 6a
xgd1-1 þ *pPZP221*	84 6 3b
xgd1-1 þ *p35S:XGD1*	102 6 4a
xgd1-1 þ *p35S:XGD1-Myc-6-His*	100 6 3a
xgd1-1 þ *p35S:*DN-*XGD1*	84 6 3b

xgd1-1 and wild-type (*qrt*) plants were transformed with the different constructs indicated and gentamycin resistant offspring grown to ma-turity. Leaves were harvested, cell wall material isolated and hydrolyzed, and monosaccharide composition determined by HPAEC-PAD. The data are expressed as the relative content of xylose in mol % (6SE, *n* ¼ 5). Numbers followed by the same letter are not significantly different (*t* test, P > 0.05). *pPZP221* is the empty vector. The wild-type phenotype is restored in mutants expressing XGD1.

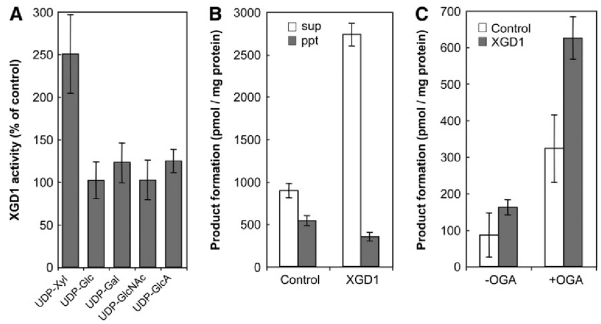

Figure 6. XGA Xylosyltransferase Activity of XGD1 Transiently Expressed in *N. benthamiana*.

XGD1 was expressed in leaves of *N. benthamiana* by *Agrobacterium*-mediated transient expression, prepared as microsomes and used for glycosyltransferase assays. Experiments were performed using duplicated samples, and the data represent mean 6 SD from two independent experiments (95% confidence interval in [A]).

(A) Enzyme reactions were performed for 4 h with the appropriate UDP-^{14}C-sugar (0.1 mM, 370 Bq) in the presence of heat-treated microsomes from noninfiltrated plants as acceptors. The products were precipitated in 70% (v/v) ethanol and analyzed by liquid scintillation counting. The bars represent the ratio of product formation between microsomes from XGD1-expressing plants and control plants. The background activities from endogenous glycosyltransferases in control microsomes were 1.1 nmol (UDP-Xyl), 2.1 nmol (UDP-Glc), 4.0 nmol (UDP-Gal), 0.7 nmol (UDP-GlcNAc), and 14 nmol (UDP-GlcNAc).

(B) Microsomes were incubated with UDP-^{14}C-Xyl (0.1 mM, 370 Bq) in the presence of heat-treated microsomes prepared from noninfiltrated *N. benthamiana* leaves. The products were precipitated in 70% (v/v) ethanol and treated with XGA hydrolase. After the treatment, ethanol was added to the reaction mixture to 70% (v/v), and the radioactivity in supernatant (sup) and in precipitate (ppt) was scintillation counted.

(C) Microsomes were solubilized and incubated 3 h with UDP-^{14}C-Xyl in the presence of oligogalacturonide mixtures of DP12-14 (OGA). The products were precipitated in 70% (v/v) ethanol and scintillation counted.

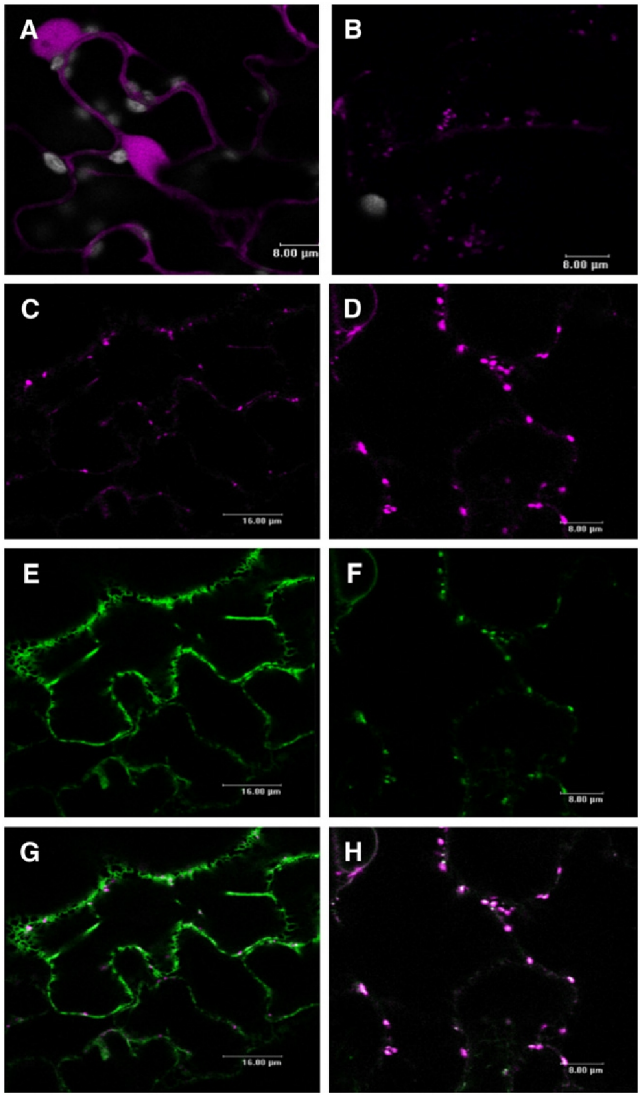

Figure 7. Subcellular Localization of Transiently Expressed XGD1-YFP in *N. benthamiana*.

N. benthamiana leaves were infiltrated with *Agrobacterium* (OD_{600} of inoculum was 0.05) carrying the constructs for expression of fluorescent proteins and observed by confocal laser scanning microscopy after 48 h.

(A) and (B) Photographs were taken for leaf specimens expressing YFP (A) and XGD1-YFP (B). YFP shows the expected cytoplasmic localiza-tion, whereas XGD1-YFP has a punctuate distribution.

(C), (E), and (G) Coexpression of XGD1-YFP and an ER marker (GFP-HDEL) where (C) and (E) represent YFP and GFP signals, shown in magenta and green, respectively, while (G) represents the merge of the two signals.

(D), (F), and (H) Coexpression of XGD1-YFP and a Golgi marker (STtmd-GFP) where (D) and (F) represent YFP and GFP signals, shown in magenta and green, respectively, while (H) represents the merge of the two. Magenta, green, and gray represent YFP, GFP, and chloroplast autofluoresence signals, respectively. Overlap of the YFP and GFP signals is shown as white (H) and is seen only with the Golgi marker.

Figure 4. Analysis of Oligosaccharides Released from Cell Walls by Digestion with XGA Hydrolase.

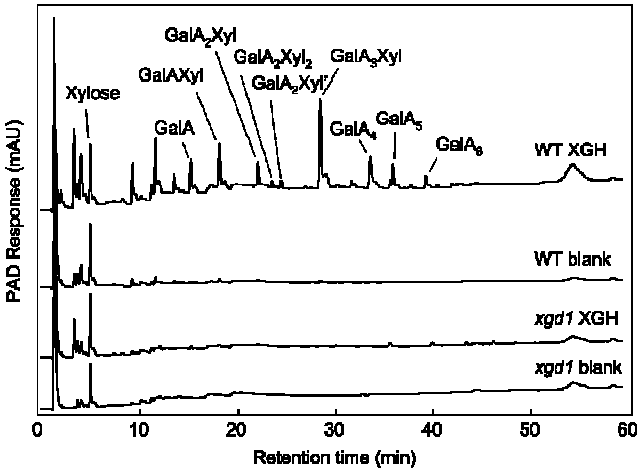

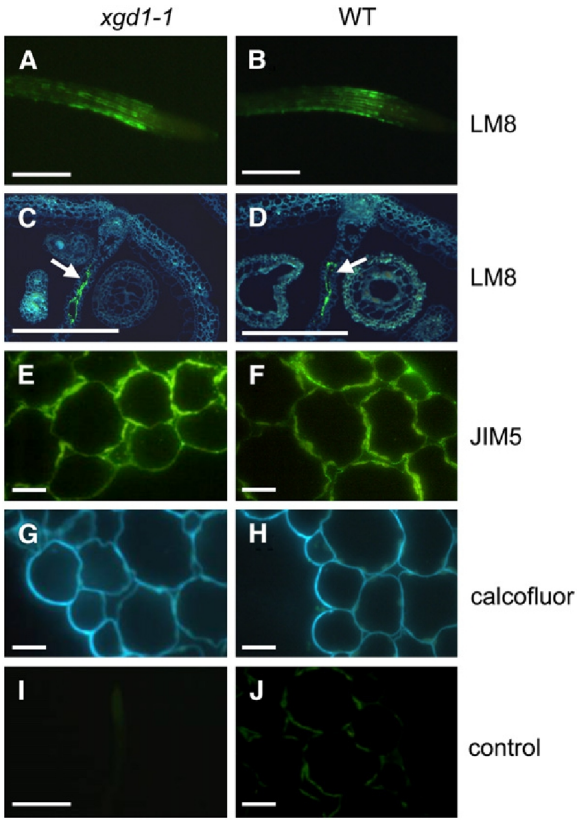

Figure 5. Immunofluorescence Analysis of Cell Wall Composition in the *xgd1-1* Mutant.

Tissues from the wild type (*qrt*) ([B], [D], [F], and [H]) and *xgd1-1* ([A], [C], [E], and [G]) were analyzed by indirect immunofluorescence label-ing. Labeling was performed on intact roots ([A] and [B]) and transverse sections of resin-embedded siliques ([C] and [D]) and leaves ([E] to [H]). Roots and siliques were labeled with an antibody with specificity for pea XGA (LM8) and leaf sections with an antibody (JIM5) with specificity for partially methylesterified HG ([E] and [F]) and calcofluor ([G] and [H]). Surface labeling of roots indicated no differences in the level of the XGA epitope recognized by LM8 between the wild type and *xgd1-1*. In siliques, the LM8 epitope was restricted to certain cells in the septum between locules (indicted by arrows), and again no differences in LM8 labeling were observed. Similarly, labeling of leaf sections with JIM5 ([E] and [F]) and staining with calcofluor ([G] and [H]) were essentially the same in the wild type and the *xgd1-1* mutant. Antibody labeling was essentially absent in controls without primary antibody of surface labeled roots (I) and leaf sections (J). Bars ¼100 mm in (A) to (D) and (I) and 10 mm in (E) to (H) and (J).